Band-gap renormalization in semiconductor quantum wells containing carriers

D. A. Kleinman and R. C. Miller
AT&T Bell Laboratories, Murray Hill, New Jersey 07974
(Received 15 February 1985)

A theoretical calculation is presented of the so-called "gap renormalization" due to free carriers for the quasi-two-dimensional (2D) electrons or holes confined in a semiconductor quantum well. A general theory of the effect is developed assuming parabolic subbands, the Hubbard approximation (random-phase approximation) for the correlation energy, and a model potential containing the well thickness for the effective 2D Coulomb interaction. Results are presented for gap renormalization versus carrier density for GaAs wells of 81 and 217 Å thickness. An experimental measurement of gap renormalization is presented which is based on an analysis of the excitation and luminescence spectra of a *p*-type modulation-doped $Ga(Ga_{1-x}Al_x)As$ multilayer sample of well width 107 Å and hole density 5.3×10^{10} cm^{-2}. The calculated value is in excellent agreement with the experimental value (6.3 meV) in this case.

I. INTRODUCTION

Despite several studies[1–3] of the quasi-two-dimensional (2D) optical spectra of semiconductor quantum wells containing carriers, particularly the GaAs wells in the $Ga(Ga_{1-x}Al_x)As$ system of heterostructures, little is known experimentally about the so-called "band-gap renormalization (BGR)" that presumably occurs in quasi-2D electron or hole systems due to an energy-lowering correlation of the free carriers. This term was originally applied[4] to the case of a 3D electron-hole plasma, the gap referring in this case to the band edges having the carriers. However, it applies also to the much more common case of a sizable equilibrium population of one type of carrier. In the case of quasi-2D spectra usually a number of gaps between the different electron and hole subbands are observed, and the question arises as to what gaps are affected by one type of carrier and by how much. By "quasi-2D" we mean that the finite thickness of the layer in which the carriers are confined must be taken into account.

In the 3D plasma case it is known[4] that the correlation effect can to a good approximation be regarded as a rigid shift of the electron and hole bands (in the region of the band edges) toward each other (hence the term "gap renormalization"). Calculations[5] for the 2D case, in the limit of zero thickness, for *n*-type Si inversion layers with only the lowest subband occupied, have also shown a nearly rigid band shift. The apparent rigid shift of the bands can be explained by the short range of the screened Coulomb interaction which samples a considerably larger region of **k** space than that occupied by the Fermi sea, making it a matter of indifference whether a recombining electron-hole pair is near the bottom or the top of the Fermi distribution. The rigid-shift picture makes possible a very simple calculation of the gap change for the plasma in terms of the derivative of the average energy per pair with respect to the carrier density.

For the quasi-2D case it is reasonable, in view of the paucity of detailed experimental information, to take over without proof the rigid-band-shift picture. Also without proof it is reasonable to assume that *all gaps* are reduced by roughly the same amount by a carrier population of either kind. Thus a population of heavy holes in the lowest hole subband is polarized by its screened interaction with any carrier, either hole or electron, causing reduction of energy. In any recombination process which removes a hole and an electron the apparent reduction of gap is the sum of the polarization energies of the electron and hole, or approximately twice the BGR computed from a consideration of the hole population alone. On the other hand, according to this view, a heavy-hole population does not cause any significant relative shift of the various heavy- and light-hole subbands, or the various electron subbands, for processes that do not involve removing an electron-hole pair.

According to our viewpoint the BGR can be detected and measured spectroscopically in quantum wells containing equilibrium carriers by looking for a single downward energy shift of all the definitely assignable features in the spectrum compared with what one expects for the same carrier density and the same well width neglecting the BGR. Ordinarily the well width L is known approximately from the growth process, but not accurately enough for evaluating the effects of carriers, so one depends on the spectrum itself to finally fix L. According to our viewpoint the BGR cancels out of the *differences* of transition energies, so if a number of transitions are observed the differences can be used to fix L.

One possible difficulty is that even if a single downward energy shift can be identified in the spectrum, it includes both the contribution of the BGR and of the exciton binding energy, since most or all the features in the spectrum are due to excitons. In a separate paper[6] the theory of quasi-2D excitons in the presence of a Fermi sea of either type will be discussed, and it will be shown that even for quite small carrier densities the exciton binding energy can be very small while the optical strength still remains observable. This suggests neglecting all exciton binding energies in carrying out the BGR analysis

described above.

An experimental BGR analysis is presented here for a modulation[7] p-doped quantum well having width $L \sim 100$ Å and hole density $N_h \sim 5.3\times10^{10}$ cm^{-2}. From a comparison of the measured excitation spectrum with the calculated spectrum neglecting exciton binding energies the sharper value $L = 107$ Å and the single shift $2E_{\rm BGR} = 12.3$ meV were determined. An analysis of an undoped sample is also presented as a control to show the soundness of the method. The success of the BGR analysis in this case tends to confirm the validity of the rigid-band-shift picture and our viewpoint of BGR. The calculated $E_{\rm BGR} = 6.0$ meV in this case agrees well with the measured value.

The quantum well has in general a number of subbands (2D energy bands for motion along the well) for electrons and holes. The theory and calculations given here neglect all but the lowest electron and hole subbands, which are assumed parabolic. Thus the carrier densities must be low enough that higher subbands are not populated. The parabolic assumption is even more restrictive in the case of holes. The upper limit on hole density depends on L, but typically for $L \sim 100$ Å the parabolic assumption is not too bad up to densities $N_h \sim 3\times10^{11}$ cm^{-2}. The results are not necessarily limited to quantum wells, but may also apply to certain cases of carrier confinement at a single interface, providing a suitable estimate for the effective L is used.

The calculations of BGR were actually performed using a program developed to compute the quasi-2D electron-hole—liquid (EHL) binding energy and equilibrium density. The results on the EHL will be reported in another paper.[8] The theory underlying this program is a straightforward adaptation to 2D of the method of Brinkman and Rice,[9] which in turn is based on the random-phase-approximation (RPA) method of Hubbard[10] for a single-component electron gas. Some of the necessary formulas for the quasi-2D case have been given by Kuramoto and Kamimura,[11] who considered the EHL in the limiting 2D case $L \to 0$. This limit, however, is rather unphysical. To treat the more interesting quasi-2D case we have used the model potential used previously[12] to discuss the biexciton in quantum wells. This potential contains a parameter which has been calibrated against L, and describes approximately the effect of finite L in reducing the 2D Coulomb interaction between particles.

II. THEORY OF SINGLE-CARRIER BGR AT ZERO TEMPERATURE

We consider a degenerate distribution of holes or electrons of density N in a quantum well occupying a parabolic subband. These particles interact through a potential[12]

$$v(r) = (1-e^{-\gamma r})/r \,,$$
$$v(\mathbf{k}) = \int dr\, v(r) e^{i\mathbf{k}\cdot\mathbf{r}} = (2\pi e^2/\epsilon_0)[k^{-1} - (k^2+\gamma^2)^{-1/2}] \,, \tag{1}$$

where γ^{-1} is a measure of the quantum-well width L which has been previously calibrated.[12] The important part of the energy per particle can be written

$$E = E_F + E_X + E_C \,. \tag{2}$$

The Fermi energy E_F is the average kinetic (or band) energy for free particles

$$E_F = (\pi\hbar^2/2m)N = \mu_F/2 \,, \tag{3}$$

where m is the mass and μ_F the chemical potential in the absence of interaction (Fermi level). The exchange energy[13] E_X is the additional contribution to the interaction energy of free particles due to antisymmetrizing the total wave function

$$E_X = -N^{-1}(2\pi)^{-4} \int\int_F d\mathbf{k}\, d\mathbf{k}'\, v(|\mathbf{k}-\mathbf{k}'|) \,, \tag{4}$$

where $\mathbf{k},\mathbf{k}'$ are restricted to the interior of the Fermi circle,

$$k < k_F, \quad \hbar^2 k_F^2/2m = \mu_F \,. \tag{5}$$

By inserting $v(k)$ from Eq. (1) and integrating first over $\mathbf{k},\mathbf{k}'$, E_X can be written

$$E_X = -(4/3\pi)(e^2/\epsilon_0)k_F[1-I(p)] \,, \tag{6}$$

where

$$I(p) = (3\pi/4)\int_0^\infty dx\, x^{-2} J_1(x)^2 e^{-px} \quad \text{when } p = \gamma/k_F \,. \tag{7}$$

For numerical evaluation it is convenient to transform $I(p)$ to the form

$$I(p) = \tfrac{3}{8}\int_0^\pi d\phi(1+\cos\phi)[(p^2+2-2\cos\phi)^{1/2} - p] \,. \tag{8}$$

$I(p)$ approaches one as p goes to zero. It is clear that $I(p)$ contains the effects of finite width.

The correlation energy E_C is given in the RPA of Hubbard[10] by

$$E_C = -\frac{\hbar}{4\pi N}\int \frac{d\mathbf{k}}{(2\pi)^2} \times \int d\omega \left[\mathrm{sgn}(\Sigma_0)\tan^{-1}\left[\frac{|\Sigma_0|}{1-A_0}\right] - \Sigma_0 \right] , \tag{9}$$

where $\tan^{-1}(\chi)$ is defined to lie in the range $0 \le \tan^{-1}(\chi) < \pi$, and $A_0(k,\omega)$ and $\Sigma_0(k,\omega)$ are defined by the RPA dielectric function

$$\epsilon(k,\omega)_{\rm RPA}/\epsilon_0 = 1 - A_0(k,\omega) - i\Sigma_0(k,\omega) \,. \tag{10}$$

General expressions for A_0, Σ_0, valid in 2D as well as 3D, are given by Hubbard.[10] The evaluation of these for the 2D case at zero temperature leads to the expressions[11]

$$\Sigma_0(k,\omega)=\frac{mv(k)}{\pi\hbar^2\chi}\left\{\left[1-\left[\frac{y+\chi^2}{2\chi}\right]^2\right]^{1/2}-\left[1-\left[\frac{y-\chi^2}{2\chi}\right]^2\right]^{1/2}\right\}\leq 0\ , \tag{11}$$

$$A_0(k,\omega)=\frac{mv(k)}{\pi\hbar^2}\left\{\left[\frac{y+\chi^2}{2\chi^2}\right]\left[1-\left[\frac{2\chi}{y+\chi^2}\right]^2\right]^{1/2}-\left[\frac{y-\chi^2}{2\chi^2}\right]\left[1-\left[\frac{2\chi}{y-\chi^2}\right]^2\right]^{1/2}-1\right\},\quad \chi=k/k_F,\quad y=2m\omega/\hbar k_F^2\ ,$$

where $[\chi]^{1/2}$ is defined to vanish for $x<0$. Hubbard[10] proposed an exchange correction to the RPA in which the quantity in large parentheses in Eq. (9) is replaced by

$$\left[\mathrm{sgn}(\Sigma)\frac{\Sigma_0}{\Sigma}\tan^{-1}\left[\frac{|\Sigma|}{1-A}\right]-\Sigma_0\right]\ , \tag{12}$$

with

$$A(k,\omega)=[1-f(k)]A_0(k,\omega)\ ,$$
$$\Sigma(k,\omega)=[1-f(k)]\Sigma_0(k,\omega)\ . \tag{13}$$

The function $f(k)$ must satisfy $f(k)\to\frac{1}{2}$ as $k\to\infty$ to take into account the fact that large k corresponds to close encounters that are forbidden by the exclusion principle when the particles have the same spin. The expression actually suggested by Hubbard is not appropriate for the 2D case as it stands, but if it is written in the more general form

$$f(k)=v[(k^2+k_F^2)^{1/2}]/2v(k)\ , \tag{14}$$

it can be applied to the 2D case.

It is convenient to write Eq. (9) in the form

$$E_C=-\frac{\hbar^2k_F^2}{2\pi m}\int_0^\infty dt_+\int_{-t_+}^{t_+}dt_-(t_+-t_-)^2\left\{\mathrm{sgn}(\Sigma)\frac{\Sigma_0}{\Sigma}\tan^{-1}\left[\left[\frac{|\Sigma|}{1-A}\right]-\Sigma_0\right]\right\}$$
$$t_\pm=(y\pm\chi^2)/2\chi\ , \tag{15}$$

noting that when $t_+>1$ the limits on t_- become ±1. The t_+ integral can be written as finite integrals

$$\int_0^\infty dt_+f(t_+)=\int_0^1 dt_+f(t_+)+\int_0^1 du\,f(u^{-1})/u^2\ . \tag{16}$$

All the finite integrals over t_-, t_+, and u can be evaluated accurately be the Gauss-Legendre numerical quadrature method.[14] From tests on exactly integrable functions qualitatively similar to Σ_0, the accuracy of these integrations can be monitored. Using a quadrature of order 12 we obtained in most cases an accuracy in E_C of four significant figures, giving an accuracy typically of three figures in E.

The chemical potential is

$$\mu=\partial(NE)/\partial N\ , \tag{17}$$

and the change in gap is defined[4] to be

$$\Delta G=\mu-\mu_F=\partial[N(E_X+E_C)]/\partial N<0\ . \tag{18}$$

This was evaluated to typically three figures from the computed values of (E_X+E_C) at five points N (spacing h) using the derivative formula

$$f'_0=(f_{-2}-8f_{-1}+8f_{+1}-f_{+2})/12h\ . \tag{19}$$

The band-gap renormalization, defined to be positive, is

$$E_{\mathrm{BGR}}=-\Delta G(N)\ . \tag{20}$$

As discussed in the Introduction, we interpret the BGR as an energy lowering due to the polarization of the Fermi sea by each particle. Any charged particle, whether belonging to the Fermi sea or not, polarizes the Fermi sea with approximately the same lowering of energy. Therefore the gap for the creation or annihilation of an electron-hole pair will appear to be reduced by approximately $2E_{\mathrm{BGR}}$. On the other hand we expect essentially no relative shift of bands for processes in which a hole or electron makes a transition between subbands.

III. CALCULATIONS OF BGR FOR GaAs QUANTUM WELLS

We use the same material constants for GaAs as were used previously[12] in discussing the exciton and biexciton. The mass m in the case of holes is the transverse heavy-hole mass called m_+ in Ref. 12. The values of m_h, m_l are relevant here only in that they determine the value of m_+. The only constants we actually use in calculating the BGR are

$$\epsilon_0=12.2,\quad m_+=0.099,\quad m_e=0.067\ . \tag{21}$$

The well-width parameter γ in Eq. (1) is shown in Fig. 1 of Ref. 12.

Calculations have been carried out giving $\Delta G(N)$ as follows: (a) holes with $L=81$ Å, (b) electrons with $L=217$ Å, and (c) electrons with $L=81$ Å. Figure 1 shows cases (a) and (b); case (c) is not shown because it lies almost exactly 6% below curve (a) over the whole range. At the high-density end the curves approximately follow a power law

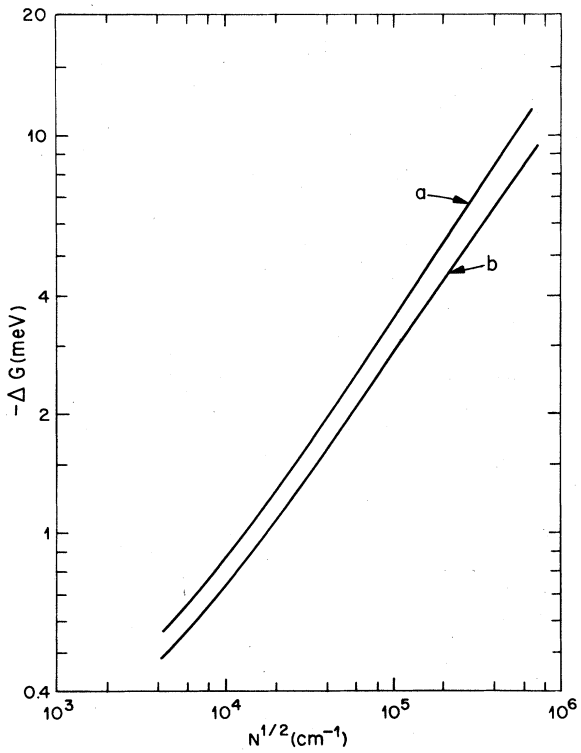

FIG. 1. The band-gap renormalization at low temperature for GaAs quantum wells containing a carrier density N (holes N_h, electrons N_e) and having well width L. (a) $N_h=N$, $L=81$ Å; (b) $N_e=N$, $L=217$ Å. Another case, (c) $N_e=N$, $L=81$ Å, is not shown but lies 6% below curve (a).

$$-\Delta G \propto N^{\alpha}, \quad \alpha \sim 0.32 . \tag{22}$$

A breakdown of the separate energy terms for case (a) is given in Table I. We believe that the results presented here are sufficient for estimating the BGR for most cases of interest that lie in the range of validity of the theory. Roughly, the criterion for N in the case of holes is that E_F should not exceed $\frac{1}{4}$ of the energy separation of the lowest heavy- and light-hole subbands (to avoid excessive nonparabolicity); in the case of electrons E_F should not exceed $\frac{1}{2}$ the separation of the lowest subbands at $k=0$ (to avoid populating the higher subband). Note that the theory should be valid for considerably higher electron densities than hole densities.

IV. DETERMINATION OF BGR FROM AN EXPERIMENTAL SPECTRUM

The modulation-doped sample to be discussed in detail was grown by molecular-beam epitaxy (MBE) with 20 periods of alternating layers (001) of 115 Å of GaAs and 153 Å $Ga_{1-x}Al_xAs$ ($x=0.44$). The center 51 Å of each barrier was doped p-type with [Be] $\sim 2\times10^{18}$ cm^{-3}, leaving 51-Å-wide undoped alloy layers next to each interface. The hole density in the GaAs quantum wells was measured by Hall effect[15] to be 5.3×10^{10} cm$^{-2}\pm$20–30%. The mobility (2350 cm^2/V sec at 4 K) was too low to permit more accurate density measurements by Shubnikov–de Haas effect.

The excitation and luminescence spectra at 5 K are shown in Fig. 2. These data were obtained using techniques described in Ref. 2 and references cited therein. The excitation spectrum was obtained with the detection set at 1.54 eV and exhibits the four exciton transitions labeled in the figure. The main exciton peaks are due to $n=1$ heavy- and light-hole excitons E_{1h} (1.5470 eV) and E_{1l} (1.5555 eV), respectively, and the $n=2$ heavy-hole exciton E_{2h} (1.6500 eV). The assignment of E_{1l} was verified by the circular polarization of this peak.[1,2] The weak "peak" labeled E_{13h} (1.606 eV) is a forbidden transition ($\Delta n=2$) that results from exciton transitions involving the $n=1$ electron and the $n=3$ heavy hole. The luminescence peak E_L occurs at 1.5430 eV on the low-energy side of E_{1h}.

For comparison as a control we show in Fig. 3 the excitation spectrum on the same energy scale of an undoped sample having nearly the same well width ($\sim$105 Å). Note in particular that compared with Fig. 2 (a) E_{1h} is stronger than E_{1l}, (b) E_{1h}, E_{1l}, and E_{2h} are all much stronger relative to the continuum level, (c) there is essentially no Stokes shift between E_{1h} and the luminescence peak, (d) there is a minimum between E_{1h} and E_{1l} that drops well below the level of the continuum beyond E_{1l}, and (e) the continua following E_{1l} and E_{2h} are approximately level like the 2D density of states. The comparisons we cite here are not limited to these two samples, but seem to be representative of p-modulation doped and undoped samples with well widths in the neighborhood of $\sim$100 Å and hole densities $N<3\times10^{11}$ cm^{-2}.

The transition energy E_T for creating an electron-hole pair of zero total momentum along the quantum well can be written

TABLE I. The energies of Eq. (2) and gap change ΔG of Eq. (18) versus density N for case (a) of Fig. 1 (holes, $L=81$ Å).

N (cm^{-2})	E_F (meV)	E_X	E_C	E	ΔG
3.3×10^{11}	4.16	−6.59	−1.74	−4.17	−11.1
1.9	2.34	−5.09	−1.79	−4.54	−9.18
1.2	1.50	−4.15	−1.77	−4.42	−7.96
0.61	0.764	−3.02	−1.69	−3.95	−6.23
0.37	0.462	−2.38	−1.65	−3.56	−5.27
0.13	0.166	−1.45	−1.45	−2.73	−3.86
4.8×10^{9}	0.060	−0.877	−1.25	−2.07	−2.73
2.5	0.031	−0.629	−1.17	−1.71	−2.28
1.2	0.015	−0.441	−0.944	−1.37	−1.82

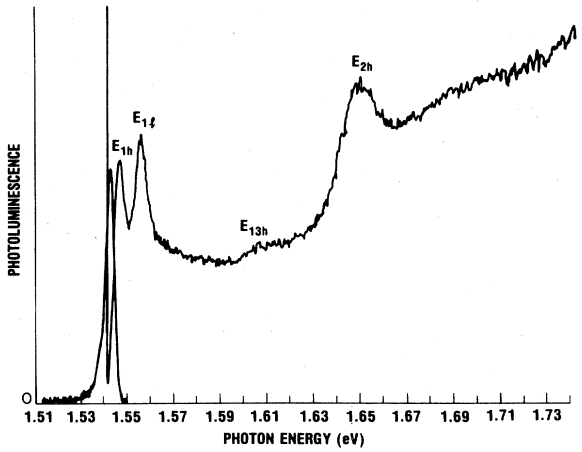

FIG. 2. Photoluminescence and excitation spectrum at 5 K for a p-type modulation-doped multi-quantum-well sample of $Ga(Ga_{1-x}Al_x)As$ with $x=0.44$, $L\sim 115$ Å, and $N_h=5.3\times 10^{10}$ cm^{-2}. Excitation intensity was ~ 0.1 W/cm^2.

$$E_T=G+W_e+W_h+F_e+F_h-B-U_e-U_h\ , \tag{23}$$

where G is the gap of the bulk material, W_e and W_h are the confinement energies of the electron and hole, respectively, in the quantum well, F_e and F_h are the kinetic energies (zero if neither carrier belongs to the Fermi sea) at the Fermi momentum k_F (regardless of which carrier forms the Fermi sea), $B>0$ is the binding energy of the exciton (or $B<0$ is the energy of an ionized "free" electron-hole state), and $U\geq 0$ is the polarization energy of a charged particle with the Fermi sea. No contribution due to space charge in the well is explicitly shown because it cancels out of W_e+W_h; however, the space-charge potential must be taken into account in the calculation of W_e and W_h. As discussed in the Introduction we shall assume that

$$U_e+U_h=-2\Delta G\ , \tag{24}$$

where $-\Delta G$ is the BGR Eq. (20) calculated for the Fermi sea alone. A recent theoretical study[6] of excitons in the presence of a Fermi sea (to be published elsewhere) indicates that B should be negligible in the present case, but the optical strength should still be sufficient to produce peaks in the spectrum (as observed). At several times higher density the E_{1h} is predicted to disappear due to the Pauli exclusion principle (as observed).[1,2]

We assume that the relevant gap in the $Ga_{1-x}Al_xAs$ barrier is the direct (Γ) gap even when the lowest gap is indirect. The gap change at the well interfaces is then given by[16]

$$G(x)-G=1.425x-0.90x^2+1.1x^3\ (\text{eV})\ ,$$
$$G=1.5192\ \text{eV}\ \ (\text{GaAs}) \tag{25}$$

and the effective masses, as represented by a linear interpolation between GaAs (Ref. 17) and AlAs (Ref. 18) are given by

$$m_e(x)=0.0665+0.0835x\ ,$$
$$m_{hh}(x)=0.34+0.175x\ , \tag{26}$$
$$m_{lh}(x)=0.094+0.069x\ ,$$

in units of the free-electron mass. The apportionment of the gap discontinuity Eq. (25) between conduction (Q_e) and valence ($1-Q_e$) bands is taken to be[17] $Q_e=0.57$. This value together with the GaAs ($x=0$) masses in Eq. (26) are consistent with both square-well and parabolic-well spectra.[17] The space-charge ("band-bending") potential for $N=5.3\times 10^{10}$ cm^{-2} and $L=107$ Å is calculated to be 1.3 meV at the center of the well; since this is rather small we shall not go into details here on the calculation of this potential. The density $N=5.3\times 10^{10}$ cm^{-2} corresponds to the sum of Fermi levels

$$F_e+F_h=3.0\ \text{meV}\ . \tag{27}$$

The quantum-well eigenvalues W_e, W_h were computed for a single well with the boundary conditions $\Psi(z)\to 0$ as $z\to\pm\infty$, and $\Psi(z)$ and $m^{-1}\Psi'(z)$ continuous at $z=\pm L/2$.

The calculated confinement energies are given in Table II for $L=107$ Å. The calculated and observed transition

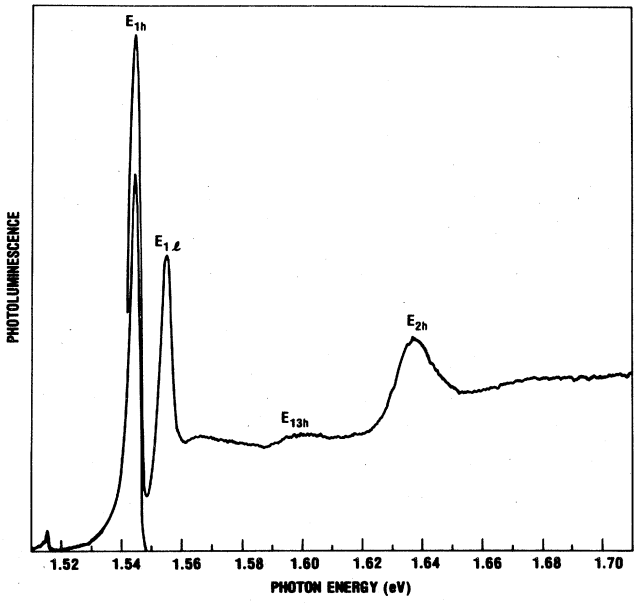

FIG. 3. Photoluminescence and excitation spectrum at 5 K for an undoped multi-quantum-well sample of $Ga(Ga_{1-x}Al_x)As$ with $L=105$ Å. The barriers were actually superlattices with average composition $x=0.24$.

TABLE II. The confinement energies W_e (electrons), W_{hh} (heavy holes), and W_{lh} (light holes) appearing in Eq. (23) calculated for $L=107$ Å relevant to the analysis of the spectrum Fig. 2.

W_e	W_{hh}	W_{lh}
27.5 (meV)	8.4	22.2
113.1	30.2	84.4
247.8	60.7	182.2
	117.0	
	179.2	

TABLE III. The analysis of the spectrum Fig. 2 for $L=107$ Å showing transition energies observed (obs), calculated (calc), the difference (calc−obs), and the deviation of (calc−obs) from its mean value 0.0123 eV.

	obs	calc	calc−obs	Deviation
E_L	1.5430 (eV)	1.5551	0.0121	−0.0002
E_{1h}	1.5470	1.5581	0.0111	−0.0012
E_{1l}	1.5555	1.5689	0.0134	0.0011
E_{2h}	1.6500	1.6625	0.0125	0.0002
		Avg. =	0.0123	
$E_{1l}-E_{1h}$	0.0085	0.0108	0.0023	
$E_{2h}-E_{1h}$	0.1030	0.1044	0.0014	
$E_{1l}-E_L$	0.0125	0.0138	0.0013	
$E_{2h}-E_{1l}$	0.0945	0.0936	−0.0009	
$E_{1h}-E_L$	0.0040	0.0030	−0.0010	

energies (omitting U_e+U_h) are compared in Table III for $L=107$ Å. The calculated E_{1h} is taken to be $E_{1h}=E_L+F_e+F_h$. Actually a number of calculations were done for various values of $L\sim 100$ Å; the value $L=107$ Å was selected to make the quantity (calc−obs) for E_{2h} equal to the average (calc−obs) for E_L, E_{1h}, and E_{1l}. This is in keeping with our viewpoint that all observed transitions should be shifted by the same amount. The differences of transitions are also given in Table III; according to our viewpoint these should not be shifted relative to the calculated values. From the average shift of 0.0123 eV we obtain the measured BGR

$$E_{\mathrm{BGR}}=6.22 \text{ meV (measured)} . \tag{28}$$

We regard the fit as satisfactory. The largest deviation of (calc−obs) from the average (calc−obs) is 1.2 meV; the largest (calc−obs) for a difference of transitions is 2.3 meV. It should be noted that if the density is increased to $N=6.8\times 10^{10}$ cm^{-2}, corresponding to the observed Stokes shift $E_{1h}-E_L=4.0$ meV, the above-mentioned deviation becomes −0.2 meV and the above-mentioned (calc−obs) becomes 1.3 meV. The calculated BGR estimated from Fig. 1 is 6.0 meV, in excellent agreement with Eq. (28).

The forbidden E_{13h} transition is not used in the analysis just given because of its breadth. The calculated value is 1.607 eV, which reduced by the average of (calc−obs) in Table III becomes 1.595 eV. This does not agree well with the E_{13h} "peak" at 1.606 but closely corresponds to the beginning at 1.597 eV of the broad E_{13h} structure. We note that the observed and calculated E_{13h} agree well without including BGR. We can not explain this anomalous behavior at the present time.

TABLE IV. Analysis of the spectrum Fig. 3 for $L=105$ Å showing the accuracy of calculated transition energies.

	obs	calc	calc−obs
E_{1h}	1.5442 (eV)	1.5433	−0.0009
E_{1l}	1.5541	1.5546	−0.0007
E_{2h}	1.6389	1.6370	0.0019
E_{13h}	1.5981	1.598	0

The spectrum Fig. 3 for the control sample is included here to show that in the absence of carriers the observed and calculated transition energies agree closely. This sample grown by MBE had GaAs wells with $L=106$ Å and barriers of $Ga_{1-x}Al_xAs$ ($x=0.24$) with $L=150$ Å with no doping. The calculated and observed transition energies are compared in Table IV. The calculated values include the exciton energies[19] for $L=106$ Å

$$B_{HH}=8.8 \text{ meV}, \; B_{LH}=10.2 \text{ meV} , \tag{29}$$

which are based on experimental observation of the exciton $2S$ excited state. Alternative values of B have been calculated[20] taking into account the penetration into the barrier, and other alternative values have been calculated[21] using a variational wave function that interpolates for all values of L between the 2D $L\to 0$ and 3D $L\to\infty$ limits. The good agreement between calculated and observed E_T in Table IV would hold regardless of which of these exciton energies B was used.

V. SUMMARY AND CONCLUSIONS

Band-gap renormalization (BGR) at low temperature in a quantum well has been studied theoretically for either electrons or holes and experimentally for the case of holes. The theory is based on the RPA method of Hubbard[10] and the model potential Eq. (1), which has previously[12] been calibrated against the well thickness L. The quantity calculated is the chemical potential Eq. (17); this can be interpreted as a change in gap ΔG given by Eq. (18) if the picture of a rigid shift of the subband is valid. It is argued that ΔG can be ascribed to the lowering of energy due to polarization of the Fermi sea by a charge carrier. According to this viewpoint any process which involves the creation or annihilation of an electron-hole pair has an apparent gap change of approximately $2\Delta G$, regardless of what subbands the pair occupies. On the other hand there is essentially no relative shift of the various electron or hole subbands for transitions that do not change the number of carriers. Our calculated results for BGN as a function of density N given by Eq. (20) are shown in Fig. 1. The various energy terms in Eq. (2) for GaAs wells are listed for a series of N values in Table I.

The excitation-luminescence spectrum for a p-type modulation-doped multi-quantum-well sample with $L \sim 100$ Å shown in Fig. 2 was analyzed according to our viewpoint of BGR. The analysis is shown in Table III for $L = 107$ Å, a value that we found gives the approximately uniform downward shift of energy of the four transitions listed. From the shift of -0.0123 eV we deduce $E_{\rm BGR} = 6.2$ meV. The forbidden transition E_{13h} was found to be anomalous for reasons not yet understood. Also analyzed as a control to check on the accuracy of transition energy calculations was the spectrum Fig. 3 for an undoped sample with $L = 105$ Å. The results are shown in Table IV.

The procedure of "fine tuning" L from the relatively rough value estimated from growth conditions is standard practice in fitting quantum-well spectra, and is justified by the fact that a number of transitions are included in the fit. According to our viewpoint of BGR one should try to find an L for samples containing carriers that fits the spectral peaks (with exciton binding neglected) except for a common shift of energy. This proved successful in the sample discussed here, and tends to confirm the correctness of our viewpoint. Also confirmed is the excellent agreement between the calculated (6.0 meV) and measured BGR (6.2 meV).

It is interesting to compare our result for GaAs(001) quantums wells with $L = 81$ Å [curve (a) of Fig. 1] to the result of Vinter[5] for Si(001) n-type inversion layers with an assumed $L = 0$. He calculated the quasiparticle self-energy using instead of the RPA dielectric function the so-called "single-plasmon-pole approximation," which is a considerable simplification that allowed the calculation to be reduced analytically to single integrals. The straight portion of our curve (a) of Fig. 1 and Vinter's Fig. 1 curve $(-M)$ can be represented by

$$-\Delta G(\text{meV}) = CN(\text{cm}^{-2})^{\alpha} ,$$
$$C = 2.1\times 10^{-3},\ \alpha = 0.36\ \text{(Vinter)} , \qquad (30)$$
$$C = 2.2\times 10^{-3},\ \alpha = 0.32\ \text{(present work)} .$$

The agreement is gratifying, but it should be mentioned that Vinter found that taking the finite thickness into account ($L \sim 30$ Å) roughly reduced C by one-half.

ACKNOWLEDGMENTS

We wish to thank A. C. Gossard and W. Wiegmann for the high-quality samples discussed here and H. L. Stormer for the Hall measurement of carrier density.

[1]R. C. Miller and D. A. Kleinman, J. Lumin. **30**, 520 (1985).
[2]R. C. Miller, P. D. Dupuis, and P. M. Petroff, Appl. Phys. Lett. **44**, 508 (1984).
[3]A. Pinczuk, J. Shah, H. L. Stormer, R. C. Miller, A. C. Gossard, and W. Wiegmann, Surf. Sci. **142**, 492 (1984).
[4]T. M. Rice, in *Solid State Physics,* edited by H. Ehrenreich, F. Seitz, and D. Turnbull (Academic, New York, 1977), Vol. 32, pp. 1–86.
[5]B. Vinter, Phys. Rev. B **13**, 4447 (1976).
[6]D. A. Kleinman, Phys. Rev. B (to be published).
[7]R. Dingle, H. L. Stormer, A. C. Gossard, and W. Wiegmann, Appl. Phys. Lett. **33**, 665 (1978).
[8]D. A. Kleinman (unpublished).
[9]W. F. Brinkman and T. M. Rice, Phys. Rev. B **7**, 1508 (1972).
[10]J. Hubbard, Proc. R. Soc. London, Ser. A **243**, 336 (1957).
[11]Y. Kuramoto and H. Kamimura, J. Phys. Soc. Jpn. **37**, 716 (1974).
[12]D. A. Kleinman, Phys. Rev. B **28**, 871 (1983).
[13]M. Combescot and P. Nozières, J. Phys. C **5**, 2369 (1972).
[14]M. Abramowitz and I. Stegun, *Handbook of Mathematical Functions* (Dover, New York, 1965), p. 887.
[15]H. L. Stormer (private communication).
[16]R. Dingle, R. A. Logan, and J. T. Arthur, Jr., in *Gallium Arsenide and Related Compounds (Edinburgh, 1976),* edited by C. Hilsum (IOP, Bristol, 1977), Chap. 4, pp. 210–215 (Inst. Phys. Conf. Ser. No. 33a).
[17]R. C. Miller, D. A. Kleinman, and A. C. Gossard, Phys. Rev. B **29**, 7085 (1984).
[18]*Semiconductors,* Vol. 17 of *Landolt-Börnstein Numerical Data and Functional Relationships in Science and Technology, Group III,* edited by O. Madelung, M. Schultz, and H. Weiss (Springer, Berlin, 1982).
[19]R. C. Miller, D. A. Kleinman, W. T. Tsang, and A. C. Gossard, Phys. Rev. B **24**, 1134 (1981).
[20]R. L. Greene, K. K. Bajaj, and D. E. Phelps, Phys. Rev. B **29**, 1807 (1984).
[21]G. Bastard, E. E. Mendez, L. L. Chang, and L. Esaki, Phys. Rev. B **26**, 1974 (1982).